

## Analytical parametrization for the shape of atomic ionization cross sections

Jan M. Rost and Thomas Pattard

Fakultät für Physik, Universität Freiburg, Hermann-Herder-Strasse 3, D-79104 Freiburg, Germany

(Received 8 August 1996)

The behavior of the ionization cross section of atoms is known classically in the limits of threshold energy and at high energies. These two limits are used to construct a simple analytical formula for the ionization cross section that depends upon two parameters: the magnitude of the maximum of the cross section and its position in energy. The parametrization has been tested for electron- and positron-impact ionization as well as for proton- and antiproton-impact ionization. It reproduces in all cases the shape of the cross section and offers a unified treatment for ionization by bare projectiles irrespectively of their charge and mass.  
[S1050-2947(97)50101-6]

PACS number(s): 34.50.-s, 34.80.-i, 82.30.-b

There has been a continuous effort to provide simple semiempirical formulas for the ionization cross section of atoms. Probably the best known formula has been given by Lotz [1]. (A summary can be found in Younger and Märk [2]; for more recent work concerning electron impact see [3].) Some of these parametrizations are rather sophisticated and incorporate the effect of the binding energy from different electron shells in a target atom. All of them have in common that they use the form of the high-energy limit with a logarithmic energy dependence  $\ln E/E$ , as results from the first Born approximation. However, the power-law behavior close to threshold—as known from the Wannier theory [4]—has not been taken into account. We will show that for a good parametrization of the cross section around its maximum, the low-energy behavior is actually more important than the high-energy behavior. For ionization by electron impact this is not too surprising since the maximum is typically located at an excess energy that equals roughly the binding energy of the ionized electron (typically 2–20 eV for valence electrons). On the other hand, the logarithmic correction becomes relevant at some keV excess energy; that is, far away from the maximum.

In the following we will therefore approximate the high-energy behavior with the simpler classical decrease, which is linear. This procedure also puts the entire parametrization on a consistent level since the low-energy power law has been derived from a classical calculation as well (although this classical low-energy limit also holds quantum mechanically [5]). Moreover, the inclusion of the threshold behavior allows one to formulate a shape function for ionization that is valid for all kinds of projectiles, from electrons over positrons to protons, antiprotons, and charged ions. For a given target, each of these projectiles leads to a different collision system with different threshold behavior to be taken into account by the shape function.

Near the threshold  $E=0$  for ionization of a neutral atom the cross section follows a power law  $\sigma(E) \propto E^\alpha$ , where  $\alpha$  depends on the final fragmented state only (e.g.,  $\alpha = 1.127$  if the final state consists of two electrons and the ionized atom, the typical situation for electron-impact ionization). The exponents can be calculated from the Wannier theory [4,6] and reflect the unstable motion away from the all-particle coalescence [7].

From the first Born approximation we know that in the high-energy limit an ionization cross section behaves as  $\ln E/E$ , whereas the classical behavior, known since 1912 [8], predicts a decrease with  $1/E$ . Since we are interested in an energy regime about the maximum of the cross section, the logarithmic term does not have a big effect and we will work with the simpler classical law.

We may combine the two limits in a natural way by writing the ionization cross section as the product

$$\sigma(E) \propto \frac{1}{E+E_0} \left( \frac{E}{E+E_0} \right)^\alpha, \quad (1)$$

where  $E$  is the excess energy of the system measured from the ionization threshold. The first factor  $(E+E_0)^{-1}$  in (1) supplies the classical high-energy limit with  $\sigma(E \gg 1) \propto E^{-1}$  (we use atomic units unless otherwise stated). The second factor, while approaching unity for large  $E$ , reduces to  $(E/E_0)^\alpha$  near the ionization threshold  $E=0$ . This is the correct form of the classical low-energy limit as derived by Wannier in 1953 [4], where  $\alpha$  depends on the collisional system.

The constant  $E_0 = E_M/\alpha$  is fixed by the maximum of the cross section,  $\sigma_M = \sigma(E_M)$ . In order to give a shape function that can be easily applied to experimental situations, we use dimensionless variables  $y = \sigma/\sigma_M$  and  $x = E/E_M$ , where  $\sigma_M$  and  $E_M$  can be determined either from theory or experiment. (The latter case amounts to fitting the cross section with two parameters,  $\sigma_M$  and  $E_M$ .) Then, Eq. (1) reads

$$y \equiv \frac{\sigma(x)}{\sigma_M} = \frac{f_\alpha(x)}{f_\alpha(1)}, \quad (2)$$

where

$$f_\alpha(x) = \frac{1}{x + \alpha^{-1}} \left( \frac{x}{x + \alpha^{-1}} \right)^\alpha. \quad (3)$$

The normalization of Eq. (2) with  $f(1)$  guarantees that  $y=1$  at the position  $x=1$  of the maximum of the cross section. Hence, the *shape* of the ionization cross section, Eq. (2), is *parameter free* and compares favorably with the experiment, as can be seen in Fig. 1(a), where the cross sec-

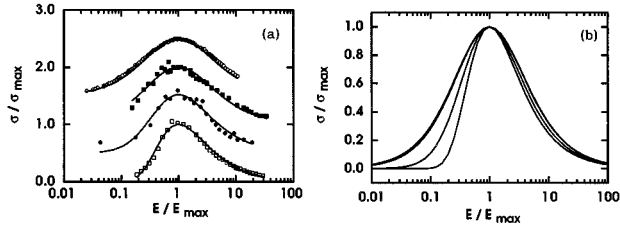


FIG. 1. (a) shows experimental cross sections for the ionization of hydrogen by various projectiles plotted in scaled coordinates  $y = \sigma/\sigma_M$  versus  $E/E_M$ . The solid line is the shape function, Eq. (2); no fit parameters are needed. Proton impact [11] is indicated by open squares and positron impact ( $y+0.5$ , [12]) by filled circles. Antiproton impact with helium as a target is shown with filled squares ( $y+1$ , [13]), and electron impact with open circles ( $y+1.5$ , [14]). (b) shows theoretical shape functions Eq. (2) for the systems of (a).

tions are plotted in the reduced units  $x$  and  $y$  together with the  $\alpha$ -dependent shape function, Eq. (2). The respective exponent  $\alpha$  determines the width of the peak in the ionization cross sections. This width becomes smaller for increasing  $\alpha$ , as can be seen in Fig. 1(b).

The novelty of Eq. (1) and Eq. (2) compared to existing parametrizations of cross sections is (i) the inclusion of the threshold behavior and (ii) the scaling of the energy in terms of  $E_M$  instead of the ionization potential  $I$  as in traditional formulas. This results in a unified view of collisions involving very different projectiles. While a good parametrization of electron-hydrogen scattering (with  $\alpha=1.127$ , see Table I) might be expected, positron-hydrogen scattering (where  $\alpha=2.65$ ) is equally well described [Figs. 2(a) and 2(b)]. Not necessarily expected is the possibility of representing the ionization of helium by antiprotons with Eq. (1), where now  $\alpha=1.199$  [Fig. 2(d)]. Most surprisingly, the proton-hydrogen ionization cross section [Fig. 2(c)] also follows Eq. (1) with an exponent of  $\alpha=69.74$ . We conclude from these observations that the inclusion of the threshold behavior is indeed important, even for the cross section far from threshold.

A closer inspection of Fig. 2(a) reveals that the shape function, Eq. (2), slightly overshoots the actual cross section at maximum. This is not observed in the other cases [Figs.

TABLE I. Examples of Wannier exponents for various collisional systems with the same potential, but different masses for projectile ( $m_p$ ) and target ( $m_T$ ).

	$m_p$	$m_T$	$\alpha$
$e^- - M_\infty$	1	$\infty$	1.127
$e^- - H$	1	1836	1.127
$e^+ - M_\infty$	1	$\infty$	2.651
$e^+ - H$	1	1836	2.650
$p^- - M_\infty$	1836	$\infty$	1.160
$p^- - H$	1836	1836	1.199
$p^+ - M_\infty$	1836	$\infty$	98.675
$p^+ - H$	1836	1836	69.74

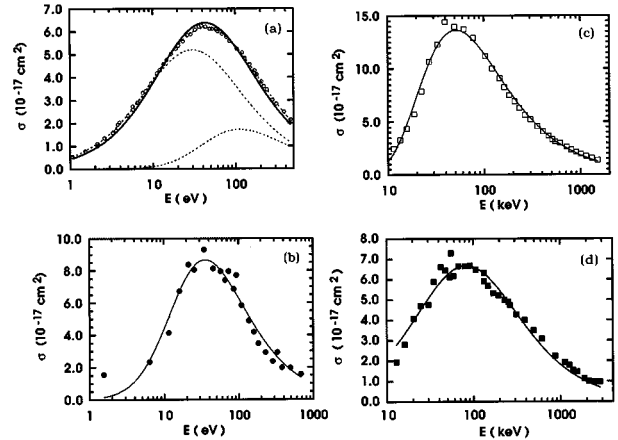


FIG. 2. Ionization of hydrogen by electrons (a), positrons (b), and protons (c). (d) shows ionization of helium by antiprotons. Symbols and experimental data are the same as in Fig. 1. The solid line is the respective cross section, Eq. (1), with  $E_M$  and  $\sigma_M$  fitted to the experimental data; for the dashed lines see text.

2(b)–2(d)]. Electron-impact ionization differs from the other three collisional systems in the indistinguishable target and projectile electrons. The Pauli principle imposes an additional symmetry that leads to two partial cross sections. They behave as  $E^\alpha$  and  $E^{3\alpha}$  close to threshold [9]. On the other hand, for high energies, symmetrization is unimportant since projectile and target electron differ very much in energy. In this situation we may extend the shape function to the form

$$f_{sym}(x) = f_\alpha(x) + \rho f_{3\alpha}(\rho x), \quad (4)$$

where  $\rho = E_M^{(\alpha)}/E_M^{(3\alpha)}$ , now a true fitting parameter, is the ratio of the maximum positions of the contributions  $f_\alpha$  and  $f_{3\alpha}$ .

The relative weight of  $f_\alpha$  and  $f_{3\alpha}$  in Eq. (4) is fixed by the requirement that both components contribute equally in the asymptotic range for large  $E$  where the ionized target and the projectile electron are distinguishable because of their large difference in velocity. Note that for Eq. (4)  $x \equiv E/E_M^{(\alpha)} = 1$  is not the position of the maximum of the cross section anymore. Figure 2(a) shows the two contributions  $f_\alpha$  and  $f_{3\alpha}$  separately; the sum—also dashed but hardly visible—fits the experimental cross section very well. It can be seen that  $f_{3\alpha}$  is indeed strongly suppressed as compared to  $f_\alpha$  close to threshold  $E=0$  and correspondingly reaches its maximum at a higher energy,  $E_M^{(3\alpha)} > E_M^{(\alpha)}$ .

For heavy-ion collisions (i.e., projectiles with masses of the order of  $10^3 m_e$  and charges  $Z \geq 1$ ),  $\alpha \approx \sqrt{\mu}$ , where  $\mu$  is the reduced mass of projectile and target in atomic units, i.e.,  $\alpha \approx 10^2$  (see Table I). Equation (3) may be simplified in this case by taking the limit  $\alpha \rightarrow \infty$ . Then we have

$$\lim_{\alpha \rightarrow \infty} f_\alpha(x) = \frac{1}{x} e^{-1/x}. \quad (5)$$

Indeed, the shape Eq. (5) (dashed curves) is indistinguishable from the shape of Eq. (3) (solid curves) with the ‘‘correct’’  $\alpha=69.7$  in Fig. 2(c). Equation (5) implies that the scaling properties of heavy-ion ionization cross sections should only

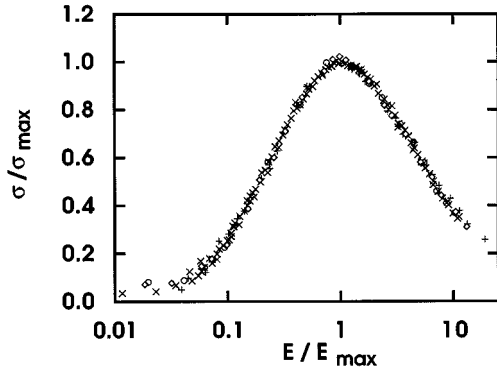


FIG. 3. Electron-impact ionization cross sections of atoms where the axes have been scaled to the respective maximum values  $\sigma_M$  and  $E_M$ . The data represent the hydrogen target ( $\circ$ ) as in Fig. 1; and from [15], helium (+), nitrogen ( $\times$ ), carbon ( $\square$ ), and oxygen ( $\triangle$ ).

depend on the position and value of the maximum of the cross section, a result that is of interest in the context of recent experiments on direct ionization by slow ions [10].

Quite generally, Eq. (3) implies identical shapes for the ionization cross section involving different targets but the same projectile. This is demonstrated in Fig. 3 for electron-impact ionization and in Fig. 4 for positron-impact ionization, respectively. The poor agreement among the positron cross sections close to the fragmentation threshold can be attributed to the difficult subtraction of the background in the experiment, i.e., positronium formation, which also produces a positive ion.

To apply Eq. (2) one needs to know the exponent  $\alpha$ , which is defined through

$$\alpha = -\frac{1}{4} + \sqrt{\frac{1}{16} + \frac{C''(\gamma_0)}{2C(\gamma_0)}}, \quad (6)$$

where  $C'' = d^2C/d\gamma^2$  with

$$C(\gamma) = \frac{Q_{13}}{\sin(\gamma_1 + \gamma)} + \frac{Q_{23}}{\sin(\gamma_2 - \gamma)} + \frac{Q_{12}}{\cos(\gamma)} \quad (7)$$

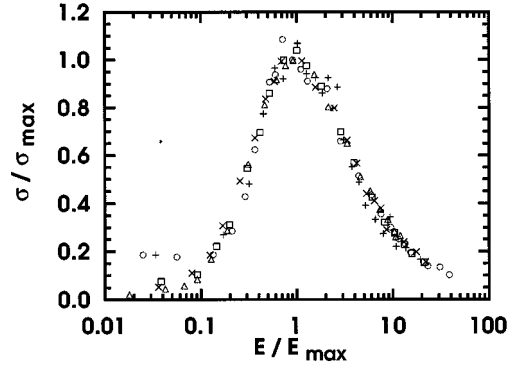


FIG. 4. Same as Fig. 3 but for positron impact. Data are for the hydrogen target (+) as in Fig. 1 and from [16] for helium ( $\triangle$ ), argon ( $\circ$ ),  $H_2$  ( $\square$ ), and for neon ( $\times$ ).

for  $-\gamma_1 < \gamma < \gamma_2$ . The angles  $\gamma_i = \arcsin[\sqrt{m_{12}m_{i3}/m_i}]$  with the reduced masses  $m_{ij} = m_i m_j / (m_i + m_j)$  between particles  $i$  and  $j$ . Finally,  $Q_{ij} = Z_i Z_j \sqrt{m_{ij}/M}$ , with  $M = \sum_{i=1}^3 m_i$  being the total mass and the particles labeled so that  $Z_1 Z_2 > 0$  holds for the respective charges  $Z_i$ . The angle  $\gamma_0$  is defined through  $C'(\gamma_0) = 0$  and must be obtained numerically unless particles 1 and 2 are identical, in which case  $\gamma_0 = 0$ . However, small differences in  $\alpha$  have little influence on the shape function, and for practical purposes it will be sufficient to use the limit of infinite mass for the target as provided in Table I.

In conclusion, based on the classical high- and low-energy limits, we have proposed a parametrization that reproduces the ionization cross section in a unified form for all kinds of projectiles. Comparing the ionization of different targets by the same projectile we have found that these cross sections have a common shape if plotted as  $\sigma/\sigma_M$  versus the scaled excess energy  $E/E_M$ . The simple shape function  $f_\alpha(x)$  applies when the ionization cross section is dominated by target electrons with the same ionization potential  $I$  so that the excess energy can be determined uniquely.

Financial support for this work by the DFG under the Gerhard-Hess-Programm is gratefully acknowledged as well as partial support from the SFB 276 at Freiburg University.

[1] W. Lotz, Z. Phys. D **206**, 205 (1967); **232**, 101 (1970).  
 [2] S. M. Younger and T. D. Märk, in *Electron Impact Ionization*, edited by T. D. Märk and G. H. Dunn (Springer, Vienna, 1984).  
 [3] H. Deutsch, K. Becker, and T. D. Märk, Int. J. Mass Spectrosc. **151**, 207 (1995).  
 [4] G. H. Wannier, Phys. Rev. **90**, 817 (1953).  
 [5] J. M. Rost, Phys. Rev. Lett. **72**, 1998 (1994).  
 [6] H. Klar, Z. Phys. A **307**, 75 (1982).  
 [7] B. Eckhardt, *Habilitationschrift* (Univ. of Marburg, Marburg, 1991).  
 [8] J. J. Thomson, Philos. Mag. **23**, 449 (1912).  
 [9] J. M. Rost, J. Phys. B **28**, 3003 (1995).  
 [10] W. Wu, C. L. Cocke, J. P. Giese, F. Melchert, M. L. A.

Raphaelian, and M. Stöckli, Phys. Rev. Lett. **75**, 1054 (1995).  
 [11] M. B. Shah, D. S. Elliot, and H. B. Gilbody, J. Phys. B **20**, 2481 (1987).  
 [12] G. O. Jones, M. Charlton, J. Slevin, G. Laricchia, À. Kövér, M. R. Poulsen, and S. Nic Chormaic, J. Phys. B **26**, L483 (1993).  
 [13] P. Hvelplund, H. Knudsen, U. Mikkelsen, E. Morenzoni, S. P. Møller, E. Uggerhøj, and T. Worm, J. Phys. B **27**, 925 (1994).  
 [14] M. B. Shah, D. S. Elliot, and H. B. Gilbody, J. Phys. B **20**, 3501 (1987).  
 [15] E. Brook, M. F. A. Harrison, and A. C. H. Smith, J. Phys. B **11**, 3115 (1978).  
 [16] H. Knudsen, L. Brun-Nielsen, M. Charlton, and M. R. Poulsen, J. Phys. B **23**, 3955 (1990).